PERIODIC SYSTEM ANALYSIS USING A LINEAR TIME INVARIANT FORMULATION

Mark Lopez (mlopez33@gatech.edu)
J.V.R. Prasad (jvr.prasad@ae.gatech.edu)
School of Aerospace Engineering
Georgia Institute of Technology
Atlanta, GA 30332, USA

Abstract

Several methods for analysis of linear time periodic (LTP) systems have successfully been demonstrated using harmonic decompositions. One method recently examined is to create a linear time invariant (LTI) model approximation by expansion of the LTP system states into various harmonic state representations, and formulating corresponding linear time invariant models. The LTI models are often significantly larger than the original system due to a large number of harmonic states retained in the LTI model. Using modal analysis, it has previously been shown that many of the harmonic states have little influence on the system dynamic modes and can be removed to form a smaller, reduced LTI model while still retaining high fidelity for the system dynamics. Gap metric analysis and additive uncertainty analysis can also be used to assess input-to-output fidelity of the reduced LTI model compared to the full LTI model. Previous results have shown that both of these methods can be used to verify that the reduced LTI models retain high input-to-output fidelity compared to the full LTI model. This paper will use the aforementioned methodology in an analysis of a full order time periodic model in addition to showing that the modal participation can be easily and accurately computed directly from the LTI.

1. NOTATION

$[\mathrm{A(t)}]$	Periodic Eigenvectors
$b_{P_i,C}$	Generalized Stability Margin of the Feedback Connection of P_i with Compensator C
c_n	Complex Fourier Coefficients
N_B	Number of Rotor Blades
N_H	Maximum Number of Harmonic Terms
N_M	Number of LTP Modes
N_S	Number of LTP States
P	Rational Transfer Function Matrix
$P^*(s)$	$= P^T(-s)$
T	Period
u	Input
$wno(g)$	Winding number of $g(j\omega)$
x	State
y	Output
δ_ν	Nu Gap Metric
η_j	System Eigenvalues
$\eta(g)$	Number of open right half plane poles of g(s)
$\eta_0(g)$	Number of imaginary axis poles of g(s)
θ_0	Collective Pitch Input
θ_{1c}	Lateral Cyclic Pitch Input
θ_{1s}	Longitudinal Cyclic Pitch Input
Λ_j	Floquet Eigenvalues
μ	Advance Ratio
$[\Phi(\mathrm{t})]$	Transition Matrix
ϕ_n	Modal Participation
Ω	Non-dimensional Rotor Speed
$\{\}$	Vector
$[\,]$	Matrix
$[-m_j-]$	Diagonal Matrix with Elements m_j
$[P,C]$	Feedback connection of P and C
$\|\cdot\|_\infty$	H_∞ norm
$()_0$	Average or 0th Harmonic Term
$()_n$	nth Complex Harmonic Term
$()_{nc}$	nth Cosine Harmonic Component
$()_{ns}$	nth Sine Harmonic Component

2. INTRODUCTION

The analysis of linear time periodic (LTP) systems is well understood using several methods. One such method is Floquet Theory, developed by Gaston Floquet [1]. This theory has been shown to provide a thorough analysis of LTP systems through the use of modal participation factors [2]. These modal participation factors describe the relative magnitude of each harmonic component for each state.

Other methods involve using a harmonic decomposition of the LTP system. One method recently examined is to create a linear time invariant model approximation by expansion of the LTP system states into various harmonic state representations and formulating corresponding linear time invariant models. Crimi and Piarulli explore the LTP system by harmonic decomposition of periodic states [3 and 4]. Prasad et al [5 – 8] use the harmonic decomposition to formulate a corresponding linear time invariant (LTI) system. This methodology provides a convenient framework,

as methods for LTI system analysis, controller synthesis and design are well developed and understood. However, previous work [7] has indicated that up to $2N_B$ harmonic terms are necessary for high fidelity. That is to say the average x_0 term and up to and including $2N_B$ harmonic terms, where "$2N_B$ harmonic terms" refers to the pair of harmonic components $x_{2N_BC}\cos(2N_Bt)$ and $x_{2N_BS}\sin(2N_Bt)$ from the harmonic decomposition of the periodic states, are necessary for high fidelity. Thus the inclusion of $2N_B$ harmonic terms makes the system size larger by $4N_s * N_B$ (2 states x_{iC} and x_{iS} for every ith harmonic term, and $2N_B$ harmonic terms). For high fidelity models, this can easily increase the number of states to be in the hundreds or thousands, drastically increasing the computational cost. However, many of those states will have very small influence and excitation, and can be excluded to reduce the system size while still maintaining high fidelity.

There are several methods previously examined for studying the fidelity of reduced order LTI models. One such method is comparison of eigenvalues. Although matching eigenvalues are necessary for high fidelity, they are not sufficient for closely matching responses [7 – 9]. A previous study [10] has evaluated the fidelity of an LTI model by comparing the modal participation factors between the LTI and LTP models, and has used the modal participation comparison as the basis for reducing the LTI size.

Once the reduced LTI model has been formed, the input-to-output fidelity of the model can then be evaluated against the full LTI model. One method to address this is comparison of response to specific inputs such as steps or sine sweeps. One problem associated with this method is that the response may not fully represent the richness in dynamics as inputs may not excite specific dynamics. Instead, use of additive uncertainty techniques [11] and gap metric analysis [12] provide ways to evaluate the input to output characteristics of the reduced LTI against the full LTI [13].

This paper is focused on using the aforementioned methodology to perform an analysis on a full order time periodic model by using a reduced order LTI approximation and comparisons of 1) time response, 2) modal participation, 3) additive uncertainty, and 4) nu gap metric.

3. METHODOLOGY

First, the LTP model must be obtained. From a nonlinear model, the LTP model can be obtained using a perturbation scheme [7] for numerical models. Second, the modal participation factors for the LTP model are obtained using the Floquet analysis. Third, the LTI model is approximated from the LTP model using the methodology presented in [7]. Next, reduced LTI models are formed using the LTP modal participation. Then the LTI modal participation is obtained using conventional eigen analysis and fidelity is evaluated by comparing it to the LTP modal participation [10]. Finally, the reduced LTI input-to-output fidelity can be evaluated using additive uncertainty and gap metric techniques [13].

3.1 Modal Participation

Once the LTP model has been obtained, the modal participation can be evaluated from the transition matrix $[\Phi(\mathrm{t})]$ and the periodic eigenvectors $[\mathrm{A(t)}]$ as shown in [2] by evaluating the following at t = T, and noting $[\mathrm{A(T)}] = [\mathrm{A(0)}]$

(1) $\left[-\exp(\eta_j \mathrm{t})-\right] = [A(t)]^{-1}[\Phi(\mathrm{t})][\mathrm{A(0)}]$

(2) $\left[-\Lambda_j-\right] = \left[-\exp(\eta_j \mathrm{T})-\right]$

(3) $\eta_j = \frac{1}{T}Log(\Lambda_j)$

The periodic eigenvectors can then be evaluated as follows

(4) $[\mathrm{A(t)}] = [\Phi(t)][A(0)][-\exp(-\eta_j t)-]$

The periodic eigenvectors are then expanded using a complex Fourier series as

(5) $A_{jk}(t) = \sum_{n=-N_H}^{+N_H} c_n \exp(in\Omega t)$

The modal participation ϕ_n for each harmonic component in each element is then calculated as

(6) $\phi_n = |c_n| \left(\sum_{n=-N_H}^{+N_H} |c_n| \right)^{-1}$

The modal participation for each element in the periodic eigenvectors is unique for a given LTP system, and will be used as the parameter for evaluating the modal participation fidelity of the LTI approximations to the LTP system. There are bookkeeping issues with the calculation of $\eta_j = \frac{1}{T}Log(\Lambda_j)$, since the logarithm is a complex logarithm, with a multivalued arctangent component. The integer added is chosen based on the application, and these issues are discussed in depth later on in the LTI Modal Participation Fidelity section.

3.2 LTI Approximation

The LTI approximation method utilized was developed in [5]. The method is based on a

harmonic decomposition of the states where x(t) are the LTP model states and x_0, x_{ic}, x_{is}, etc., are the LTI model states.

$$(7)\quad x(t) = x_0 + \sum_{n=1}^{N_H} x_{nc}\cos(nt) + x_{ns}\sin(nt)$$

(8)

$$\{x_{LTI}\} = \left\{x_0^T \ldots x_{ic}^T\, x_{is}^T \ldots x_{jc}^T \ldots \dot{x}_0^T \ldots \dot{x}_{ic}^T\, \dot{x}_{is}^T \ldots \dot{x}_{jc}^T\, \dot{x}_{js}^T \ldots\right\}^T$$

$$(9)\quad \{x_{LTI}\} = \left\{x_{disp,LTI} \quad x_{vel,LTI}\right\}^T$$

$\{x_{LTI}\}$ is comprised of the harmonic terms of displacement states and their first time derivatives. A similar expansion is done for the inputs $u(t)$ and the outputs $y(t)$ to formulate the corresponding $\{u_{LTI}\}\ and\ \{y_{LTI}\}$. It should be noted that while the modal participation calculation is done using complex harmonic coefficients, the LTI states use the trigonometric harmonic coefficients. Also, for a true representation of the LTP system, the LTI approximation would require an infinite number of harmonic terms and therefore an infinite dimensional system. This infinite dimensional system however, can be approximated by a finite dimensional one, since many of the terms will be near zero. It is suggested that for sufficiently high accuracy for vibration analysis, at least $2N_B$ harmonic terms are necessary (i.e. for a 4 bladed rotor $N_H = 2N_B = 8$) [7]. The LTI system can then be formed as follows

$$(10)\quad \{\dot{x}_{LTI}\} = \begin{bmatrix} F_{11} & F_{12} \\ F_{21} & F_{22} \end{bmatrix}\{x_{LTI}\} + \begin{bmatrix} G_1 \\ G_2 \end{bmatrix}\{u_{LTI}\}$$

$$(11)\quad \{y_{LTI}\} = \begin{bmatrix} H_1 \\ H_2 \end{bmatrix}\{x_{LTI}\} + [E]\{u_{LTI}\}$$

The formulations for each element for each matrix are presented in closed form in [7].

3.3 LTI Model Analysis

Once the previous steps have been completed, the LTI model analysis can begin. First, various LTI model reductions are formed based on the LTP modal participation. Reductions are formed by retaining LTI states corresponding to LTP harmonic components with significant modal participation. Next, the modal participations of the reduced LTI models are determined by calculating the eigenvectors which correspond to the trigonometric Fourier coefficients of the periodic eigenvectors. Then converting the eigenvectors from trigonometric Fourier coefficients to complex Fourier coefficients, the modal participation can be calculated in the same manner as the periodic eigenvectors using the same formulation, and taking any harmonic coefficients that were not included to be zero.

3.4 LTI Model Reduction

The LTI model formed by the previous LTI model approximation method utilizes the harmonic decomposition of the each LTP state, including each harmonic term from 0 to $2N_B$. For many cases however, the harmonic states with little excitation can be approximated as 0 and left out entirely from the LTI model while still maintaining high fidelity. The choice of which harmonic states to retain is given by the modal participation of the LTP system. LTI states with the highest corresponding LTP modal participation are retained, and LTI reductions are formed by excluding LTI states with corresponding small LTP modal participation. In general, reductions are formed by either of two ways: by starting with the fully expanded LTI model and then excluding the corresponding lowest modal participation harmonic states to reduce the size of the model; or starting with the highest modal participation harmonic states and including the next higher modal participation harmonic states, thus progressively increasing the size of the model.

Frequently, the harmonic decomposition is only necessary for the periodic states, and the non-periodic states will only require the average or 0^{th} harmonic term. For a helicopter this means that the rotor states are fully decomposed while the body and inflow states require only 0^{th} harmonic terms. Further reductions to the LTI are formed excluding specific rotor harmonic states beginning with those corresponding to the lowest LTP modal participation.

3.5 LTI Modal Participation

The modal participation for each state is unique to each system. Thus, if the modal participation for an LTI model approximation can be calculated and shown to be the same as the modal participation for the original LTP system, the LTI model can be considered a good approximation for the LTP system. The steps to calculate modal participation factors of a LTI model follow similarly to the LTP modal participation, with a few bookkeeping changes to keep in mind.

The modal participation for each harmonic component for a given LTP state is given by the magnitude of the harmonic (Fourier) coefficient divided by the sum of the magnitudes for all harmonic component coefficients of the given state. The Fourier coefficients for the LTI model are found by solving for the eigenvalues and eigenvectors of the LTI model. The Fourier coefficients for each LTP state are then directly given by the corresponding harmonic states in the LTI model eigenvectors. It is important to note however, that the LTP modal participation relies on a complex Fourier series expansion, thus the LTP model harmonic terms and harmonic coefficients are in complex form. The LTI expansion uses

trigonometric harmonic terms and harmonic coefficients, and will first need to be transformed into complex form. The transformation between complex and trigonometric harmonic coefficients using the previous decomposition nomenclature is as follows

From complex to trigonometric

(12) $x_0 = c_{+0}$

(13) $x_{nc} = c_{+n} + c_{-n}$

(14) $x_{ns} = i(c_{+n} - c_{-n}) = \frac{c_{-n} - c_{+n}}{i}$

From trigonometric to complex

(15) $c_{+0} = x_0$

(16) $c_{+n} = \frac{x_{nc} - i x_{ns}}{2}$

(17) $c_{-n} = \frac{x_{nc} + i x_{ns}}{2}$

Once the LTI model eigenvalue problem has been solved and the eigenvectors have been transformed from trigonometric form to complex form, the modal participation for the LTI model can be computed in exactly the same manner as the LTP model. It is worth noting that for any harmonic states that have been removed, their harmonic coefficients are considered to be zero and thus have a corresponding zero modal participation. It is also worth noting that similar to the LTP modal participation each LTI harmonic coefficient magnitude is divided by the sum of all harmonic component magnitudes. Thus, the LTI modal participation of a selected harmonic component of a system state is determined directly by using the eigenvector elements of the LTI model.

3.6 LTI Modal Participation Fidelity

The fidelity of each LTI model reduction is assessed by comparing the LTI modal participation with the LTP modal participation. However, there can be confusion as to which LTI mode should be compared to which LTP mode. As the LTP has N_S states, it also has N_S corresponding modes; however, the eigenvalues associated with these modes are not unique. Although Ref. 2 addresses this issue by showing that the choice of integer added to the Floquet exponent is arbitrary, the integers chosen for this analysis and the examples presented later on are first constrained by the LTI model, as it will only have a set number of corresponding eigenvalues, i.e., the LTI model does not include the infinitely many eigenvalues given in the LTP analysis, since there is no bookkeeping integer choice in the LTI eigen-analysis. The choice of integers is made to follow conventional rotorcraft analysis, where body and inflow modes are kept at 0/rev (the exponent added is 0), while rotor modes have eigenvalues at various frequencies. For example, for a 4 bladed rotor eigenvalue integers are chosen to correspond to the conventional coning, nutation, precession, and differential modes. Once the LTP eigenvalues and modes have been decided, the only LTI modes to be compared are the ones with eigenvalues matching the LTP base eigenvalues.

The error for each LTI model is calculated by taking the weighted sum of the absolute value of the difference of modal participations for each harmonic for a given state, and taking the average of that value for each rotor displacement state and each mode. The modal participation fidelity for each LTI model is then calculated as 1 minus the modal participation error:

(18) $$Modal\ Participation\ Error = \sum_{j=1}^{N_S} \frac{1}{N_S} \sum_{i=1}^{N_M} \frac{1}{N_M} \sum_{n=1}^{N_H} \left|\phi_{LTP,n} - \phi_{LTI,n}\right| \phi_{LTP,n}$$

(19) $$Modal\ Participation\ Fidelity = 1 - Modal\ Participation\ Error$$

There are several things worth noting at this point about the calculation. First, the error only includes rotor displacement states. Hence it does not include body, inflow, and rotor velocity states. This is done because as noted previously, in many cases the body and inflow states are not decomposed under the assumption that they exhibit very negligible periodicity and thus would have negligible effects on the error. Furthermore, the error calculated has already been normalized since the modal participation is a normalized parameter, i.e. error of 0 corresponds to an exact match and 1 corresponds to 100% error. The LTP modal participation factor outside of the absolute value factor is a weighting term which puts the heaviest weight on highest participating harmonic components.

3.7 LTI Reduction Selection

At this point the analysis of various LTI reductions has been completed, and the only remaining step is selection of a specific LTI reduction. This choice is done by selecting the lowest fidelity LTI reduction which is higher than the chosen desired fidelity over the range of advance ratios considered. If the LTI reductions were created properly, the lowest LTI meeting the desired fidelity

criteria would be the smallest sized system with the least number of LTI states.

Graphically, the process is to create a plot of each LTI reduction fidelity for the range of advance ratios considered. The LTI reduction selected is then chosen as the LTI reduction which lies above and closest to the desired fidelity.

3.8 Additive Uncertainty Analysis

Although for the examples presented in this paper the LTI reduction was formed using the methodology previously described, all of the input-to-output fidelity analysis described in this paper can be performed to compare any full and reduced LTI models irrespective of how the reduced LTI model was formed from the full LTI model. In fact, one could use the input-to-output fidelity as a basis for the LTI model order reduction itself. However, in this study the modal participation criterion is first applied to obtain a reduced order LTI model and then the resulting reduced LTI model is analyzed for input-to-output model fidelity.

Once an LTI reduction has been selected, the input-to-output fidelity of the reduced LTI model can be compared to the full LTI model by considering the normalized additive error to be the normalized additive uncertainty [11]. The full LTI model is considered as the truth model and the reduced LTI model is considered as the approximation. Additive uncertainty is used due to the fact that the truth model is known. The normalized additive error is calculated for a single input and a single output. The normalized error is then calculated as the H_∞ norm of the difference between the full and reduced LTI models normalized by the H_∞ norm of the full LTI model.

$$(20)\quad Normalized\ Additive\ Error = \frac{\|P_1 - P_2\|_\infty}{\|P_1\|_\infty}$$

Where,

P_1 is the full LTI model transfer function
P_2 is the reduced LTI model transfer function
$\|\cdot\|_\infty$ is the H_∞ norm

The transfer functions and the normalized additive error are for a single input and single output (SISO). Thus the normalized additive error can be computed for particular input-to-output mappings. The normalized additive error is then interpreted to be a measure of the percentage difference between the full and reduced LTI models for a particular input-to-output mapping. A small error corresponds to full and reduced LTI models being close. The additive uncertainty value so obtained can form the basis for additional controller robustness to be considered in the design process.

3.9 Gap Metric Analysis

The nu gap metric is used to evaluate the change in generalized stability margin between the full and reduced LTI systems [12]. Like the normalized additive error, the nu gap metric is computed for a single input and a single output. The nu gap metric δ_ν can be computed for a single input and single output as follows, if a winding number condition is satisfied:

$$(21)\quad \delta_\nu(P_1, P_2) = \sup_\omega \frac{|P_1(j\omega) - P_2(j\omega)|}{\sqrt{1+|P_1(j\omega)|^2}\sqrt{1+|P_2(j\omega)|^2}}$$

If the winding number condition is not satisfied, then $\delta_\nu(P_1, P_2) = 1$. The winding number condition for $\delta_\nu(P_1, P_2) < 1$ can be formulated as in Equations (22) and (23):

$$(22)\quad \det(I + P_2^* P_1) \neq 0\ \forall\omega$$

$$(23)\quad wno\ \det(I + P_2^* P_1) + \eta(P_1) - \eta(P_2) - \eta_0(P_2) = 0$$

Where $P^*(s) = P^T(-s)$ for real rational $P(s)$ which is the case here. Here, the winding number condition is formed into the requirement of both Eqs. (22) and (23) to be satisfied for $\delta_\nu(P_1, P_2) < 1$.

The nu gap metric is a number from 0 to 1 where 0 corresponds to the models being close (Ref. 12). It is bounded from above by the gap metric δ_g (Ref. 12), which can be useful if there is numerical difficulty in calculating the nu gap metric. The nu gap metric relates the generalized stability margins through the following inequality:

$$(24)\quad \arcsin b_{P_2,C} \geq \arcsin b_{P_1,C} - \arcsin \delta_\nu(P_1, P_2)$$

where $b_{P_i,C}$ is the generalized stability margin of the feedback connection of P_i with compensator C, $[P_1, C]$.

It is clear from the relation that if the nu gap metric between P_1 and P_2 is small, then any compensator designed to stabilize P_2 will also stabilize P_1 since the change in generalized stability margin will be small. It is common to consider that a gap metric less than 1/3 corresponds to the models being close. Any input-to-output mappings with small nu gap metrics would be good candidates for closing loops for feedback. Any input-to-output mappings with comparatively larger nu gap metric would need additional stability margin designed into the compensator for closing feedback loops.

3.10 Additive Uncertainty versus Gap Metric Analysis

It is important to note that although both types of analyses measure differences in the input-to-output characteristics of two systems, the characteristics that they measure are not the same. The nu gap metric is a measure of the loss of stability margin between the two systems, and thus is related to the closed loop behavior of the two systems. The additive uncertainty analysis is associated only with the open loop behavior of the two systems, and hence, can provide a basis for additional controller robustness to be considered in the design process. A small normalized additive error would indicate that the open loop behaviors of the two systems are similar. On the other hand, a small nu gap metric indicates that there is minimal change in generalized stability margin, thus closed loop behaviors of the two are similar; that is to say, any controller that stabilizes one will also stabilize the other. It has been shown in [12] that closeness in one measure does not imply the closeness in the other measure, thus both should be considered to evaluate the full input-to-output characteristics.

4. NUMERICAL EXAMPLES

4.1 Full Order Generic Helicopter Model

This example utilizes the nonlinear FLIGHTLAB generic helicopter model, which includes 6 rigid body degrees of freedom, Peters-He 15 state inflow, and coupled elastic blade flap-lag degrees-of-freedom of a four-bladed rotor. This model is linearized at each azimuthal position to form the LTP. The inflow model is quasi-statically reduced from 15 states to 3, removing the very high frequency apparent mass effects whose contributions to higher harmonic hub vibration are very small. The linearized model includes 47 LTP states comprised of: 8 body states; 3 inflow states; and 32 rotor states consisting of 16 rigid flapping and lead lag, and 16 elastic flapping and lead lag. The rotor radius is 26.83 feet, the rotor speed is 27 radians per second, and the model is linearized at advance ratios from 0 to 0.35.

The body and inflow states are retained to keep the richness in rotor dynamics associated with those states, but only include the average harmonic terms for each in the LTI model. The rotor states are decomposed and include up to 8 harmonic terms for the full LTI model, resulting in a size of 555 LTI states (544 rotor, 8 body, and 3 inflow states).

The LTP and full LTI models are verified against the nonlinear model using comparisons of time responses to generic inputs. Figures 1 to 6 show the time histories of each model in response to a 4/rev chirp inputs. Figures 1 and 2 compare the responses for a 4/rev collective chirp, Figs. 3 and 4 compare the responses for a 4/rev lateral cyclic chirp, and Figs. 5 and 6 compare the responses for a 4/rev longitudinal cyclic chirp. These chirp inputs excite much of the behavior due to the varying frequency of the input. The normalized root mean squared errors defined by Eqn. (25) for each LTP and LTI response compared to the nonlinear model are shown in Table 1.

(25) $$Normalized\ RMS = \frac{1}{y_{NL,max} - y_{NL,min}} \sqrt{\frac{1}{n}\sum_{i=1}^{n}\left(y_{NL,i} - y_{Lin,i}\right)^2}$$

Each RMS is small for each force/moment output and each chirp input both for LTP and LTI models, hence both LTP and full LTI models are considered to be accurate to the original nonlinear model.

4.2 Modal Participation Evaluation

The Floquet analysis (including up to the 8th harmonic term for modal participation) of the LTP system clearly indicates that isolated harmonic terms for each degree of freedom contain nearly all of the dynamics for the system. Throughout the advance ratio range the differential rotor states modal participations primarily include only the 2nd harmonic term, with the 6th harmonic term being the next highest. This is shown in Figs. 7 and 8 for rigid and elastic flapping respectively for one mode at an advance ratio of 0.25. The remaining rotor states include primarily only the 0th and 4th harmonic terms, followed by the 8th harmonic being the next highest. Examples for rigid and elastic coning angles are given in Figs. 9 and 10, respectively. This is similar to previous results found with lower fidelity models (Ref. 10).

Forming an LTI reduction using only the 2nd harmonic term for differential rotor states, and 0th and 4th harmonic terms for each of the other rotor states yields a total of 99 reduced LTI states (referred to as LTIr 3 in figures). This may be sufficient for many applications, however retaining the 2nd and 6th harmonics for the differential rotor states and the 0th, 4th and 8th harmonic for all of the other rotor states provides better modal participation fidelity although it increases the total reduced LTI states to 163 (referred to as LTIr 2 in figures). Furthermore, retaining all 0th and even numbered harmonics (2, 4, 6, and 8) for all of the rotor states, increases the system size to 299 reduced LTI states but also marginally increases the fidelity (referred to as LTIr 1 in figures).

The modal participation is determined directly for the LTI full and reduced LTI approximations. Figures 7 through 10 compare the modal participations for the LTP, full LTI, and the previous 3 reduced LTI models for a single mode at

a single trim condition. Figures 7 and 8 show that each of the LTI approximations have nearly the same modal participation for -2 and +2 harmonics as the LTP for the rigid and elastic flapping differential states, although the accuracy does marginally degrade with the lower order LTI approximations. Figures 9 and 10 both show that all of the LTI approximations accurately reflect the +0, -4, and +4 modal participations for the rigid and elastic flapping coning states, again with the accuracy marginally degrading with the decrease in model order for the LTI approximations shown.

Figure 11 shows the total modal participation fidelity for each LTI approximation throughout the entire range of advance ratios. From Fig. 11, it is clear that the reduced LTI approximations all have very high levels of fidelity. Thus, it is clear that all of the odd numbered harmonic terms (1st, 3rd, 5th, and 7th) have very little excitation and contribution to the model fidelity. Thus, most of the excitation occurs in the 0th and even numbered harmonic terms. Furthermore, as demonstrated by the modal participation fidelity of LTIr2 and LTIr3, only every other even harmonic largely contributes for a particular LTP state. That is, 2nd and 6th harmonic terms are dominant for differential rotor states, while 0th, 4th, and 8th are the primary contributors for the other rotor states.

It is clear from Fig. 11 that the modal participation for the three highest fidelity LTIs closely reflects the LTP modal participation. Also, because the LTIs have only finitely many harmonics included, there are no bookkeeping issues related to the eigenvalues and nomenclature of harmonics terms. Thus, it is clear that with a sufficient fidelity LTI, the modal participation can be easily and accurately calculated from an LTI approximation.

Although 3 different LTI reductions have been shown to be accurate to the LTP model with varying levels of fidelity while being much smaller than the full LTI at 555 states, the LTI reduction to be further used in input output analysis is LTIr2 with 163 states. Although the 8th and 6th harmonic terms have much smaller modal participations in comparison to the 0th and 4th, and 2nd harmonic terms respectively, they are still much more important than any of the other harmonic terms and will be retained in the input-to-output model fidelity evaluations.

4.3 Input-to-Output Model Fidelity Evaluation

For input-to-output model fidelity evaluation, it is important to consider the inputs and outputs for the model. The generic helicopter model includes the conventional swashplate cyclic, and collective inputs as well as higher harmonic control (HHC). HHC can be done directly through harmonic inputs of the swashplate. That is to say, a nth harmonic input can be inputted to either the collective, lateral cyclic, or longitudinal cyclic for the purposes of HHC. Specifically, this can be done by harmonic decomposition of each of the inputs as follows:

(26)

$$\theta_0 = (\theta_0)_0 + \sum_{n=1}^{N_H} [(\theta_0)_{nc} \cos(\Omega t) + (\theta_0)_{ns} \sin(\Omega t)]$$

(27)

$$\theta_{1s} = (\theta_{1s})_0 + \sum_{n=1}^{N_H} [(\theta_{1s})_{nc} \cos(\Omega t) + (\theta_{1s})_{ns} \sin(\Omega t)]$$

(28)

$$\theta_{1c} = (\theta_{1c})_0 + \sum_{n=1}^{N_H} [(\theta_{1c})_{nc} \cos(\Omega t) + (\theta_{1c})_{ns} \sin(\Omega t)]$$

Where $(\theta_0)_0$ is the average, and $(\theta_0)_{nc}$ and $(\theta_0)_{ns}$ are the nth cosine and nth sine components respectively of the collective input. Similarly, $(\theta_{1s})_0$, $(\theta_{1s})_{nc}$, $and (\theta_{1s})_{ns}$ are the average, nth cosine, and nth sine components of the longitudinal cyclic input; and also $(\theta_{1c})_0$, $(\theta_{1c})_{nc}$, $and (\theta_{1c})_{ns}$ are the average, nth cosine, and nth sine components of the lateral cyclic input.

The LTI approximations include all 0th through 8th harmonic components of the hub shears and moments. For the purpose of vibration reduction only the 4th harmonic inputs and outputs would be most relevant. Thus, only the 4th harmonic inputs and outputs are considered in the results presented here.

For the purposes of controller design, the swashplate input transfer functions that represent the direct axis transfer functions are the input-to-output mappings of interest. It is well known that the swashplate input direct axis transfer functions are those from collective to Fz, collective to Mz, lateral cyclic to Fy, lateral cyclic to Mx, longitudinal cyclic to Fx, and longitudinal cyclic to My. For the purposes of control design for vibration reduction, the swashplate transfer functions considered here will be focused on the direct axis transfer functions from 4/rev inputs to 4/rev outputs.

The normalized additive error is calculated for all direct axis 4/rev swashplate input to 4/rev output transfer functions. In particular the normalized additive error is shown on Figs. 12 and 13 for 4/rev collective to 4/rev Fz and 4/rev Mz transfer functions with results that are representative of all the direct axis transfer functions examined. Figures 12 and 13 show clearly that 4/rev collect direct axis transfer functions and in fact all direct axis transfer functions have extremely small normalized additive errors, below 10^{-4} for each transfer function throughout the range of advance ratios. Thus, controller designs based on 4/rev

inputs to 4/rev direct axis outputs need no additional robustness to be considered.

The nu gap metric is calculated for all direct axis 4/rev swashplate input to 4/rev output transfer functions. The nu gap metric for 4/rev collective input to 4/rev Fz and 4/rev Mz is shown on Figs. 14 and 15, where the results are representative of all the direct axis transfer functions examined. Figures 14 and 15 show that the 4/rev collective direct axis transfer functions and in fact all direct axis transfer functions have extremely small nu gap metrics, below 10^{-3} for each transfer function throughout the range of advance ratios. Thus, all of the direct axis transfer functions have little losses in generalized stability margin. This indicates that each of the direct axis transfer functions would be viable candidates for use in feedback control design.

Thus, both the nu gap metric and normalized additive error show similar results for 'which transfer functions would be viable for use in controller design'. Small normalized additive error is associated with the open loop responses of the transfer functions being close, while small nu gap metric is associated with the closed loop responses of the transfer functions being close. The results have shown that the all of the 4/rev swashplate direct axis transfer functions show similar open loop and closed loop input-to-output characteristics, and would be viable candidates for use in HHC controller design.

The results presented here for LTIr2 for the full order GHM are different from those of [13] for the reduced order GHM. In [13], an LTI reduction considering only the 2^{nd} harmonic terms for differential states, and 0^{th} and 4^{th} harmonic terms for other rotor states were considered. This reduced LTI was shown to have significant losses in fidelity for 4/rev lateral cyclic to 4/rev Fy, and 4/rev longitudinal cyclic to 4/rev Fx, and hence those transfer functions were not good candidates for use in HHC controller design. The difference here is that the inclusion of additional higher harmonic terms (6^{th} for differential rotor states and 8^{th} for other rotor states). The inclusion of the additional higher harmonic terms in LTIr2 is what substantially increase the fidelity of the 4/rev lateral cyclic to 4/ref Fy, and 4/rev longitudinal cyclic to 4/rev Fx transfer functions, compared to the full LTI which includes all 0^{th} up to 8^{th} harmonic terms for all of the rotor states. Hence, for LTIr2 for the full order GHM, all of the direct axis transfer functions considered have very high fidelity to the full LTI and are good candidates for controller design.

5. SUMMARY AND CONCLUSIONS

It has previously been shown how to compute the fidelity of an LTI approximation for an LTP system using modal participation. The modal participation can then be used to form a reduced LTI model. It has been shown here that in particular LTI models with sufficient high fidelity can be used to extract modal participation directly. This LTI modal participation extraction method avoids any ambiguity associated with bookkeeping issues in traditional Floquet analysis. This can be done even with reduced LTIs approximations while still maintaining high fidelity.

For the full order FLIGHTLAB generic helicopter model with 15 state inflow and elastic blade considered, 3 different LTI reductions have been shown to have high fidelity. In particular, retaining only the 2^{nd} and 6^{th} harmonic terms for the differential rotor states, and 0^{th}, 4^{th} and 8^{th} harmonic terms for each of the other main rotor states retains nearly all of the fidelity of the full LTI model that includes the 0^{th} up to 8^{th} harmonic terms, while being less than a third half the size. This high fidelity has been shown both in terms of modal participation characteristics, as well as input-to-output characteristics through the normalized additive error and nu gap metric. Specifically, this reduction maintains nearly all of the modal participation fidelity of the full LTI throughout the advance ratios considered in addition to having all direct axis transfer functions as good candidates for controller design.

The methodology discussed demonstrates an alternative method for modal participation evaluation through reduced order LTI models, as well as fidelity evaluation of those reduced order LTI models. The results demonstrated thus far have been applied to high fidelity full order generic articulated helicopter. Thus, it is recommended these techniques be studied with other vehicle configurations, such as co-axial rotorcraft or compound rotorcraft.

6. ACKNOWLEDGMENTS

This study is funded by the U. S. Army under the Vertical Lift Research Center of Excellence (VLRCOE) program managed by the National Rotorcraft Technology Center, Aviation and Missile Research, Development and Engineering Center under Cooperative Agreement W911 W6-11-2-0010 between the Georgia Institute of Technology and the U. S. Army Aviation Applied Technology Directorate. The authors would like to acknowledge that this research and development was accomplished with the support and guidance of the NRTC. The views and conclusions contained in this document are those of the authors and should not be interpreted as representing the official policies, either expressed or implied, of the Aviation and Missile Research, Development and Engineering Center or the U.S. Government.

7. REFERENCES

1. Floquet, G., “Sur les équations différentielles linéaires à coefficients périodiques”, Ann. École Norm. Sup. 12: 47-88, 1883.
2. Peters, D.A., Lieb, S.M., “Significance of Floquet Eigenvalues and Eigenvectors for the Dynamics of Time-Varying Systems”, 65th Annual National Forum of the American Helicopter Society, Grapevine, Texas, May 27-29, 2009.
3. Crimi, P., “A Method for Analyzing the Aeroelastic Stability of a Helicopter Rotor in Forward Flight”, NASA-CR-1332, August 1969.
4. Piarulli, V. J. and White, R. P., Jr., “A Method for Determining the Characteristic Functions Associated with the Aeroelastic Instabilities of Helicopter Rotor Blades in Forward Flight,” NASA CR-1577, June 1970.
5. Prasad, J.V.R., Olcer, F.E., Sankar, L,N. and He, C., “Linear Models for Integrated Flight and Rotor Control,” Proceedings of the European Rotorcraft Forum, Birmingham, UK, September 16-18, 2008.
6. Prasad, J.V.R., Olcer, F.E., Sankar, L.N., He, C., “Linear Time Invariant Models for Integrated Flight and Rotor Control,” 35th European Rotorcraft Forum, Hamburg, Germany, September 22-25, 2009.
7. Olcer, F.E., “Linear Time Invariant Models for Integrated Flight and Rotor Control,” Doctor of Philosophy Thesis, Georgia Institute of Technology, July 2011
8. Olcer, F.E and Prasad, J.V.R., “A Methodology for Evaluation of Coupled Rotor-Body Stability using Reduced Order Linear Time Invariant (LTI) Models,”, 67th Annual National Forum of the American Helicopter Society, Virginia Beach, Virginia, May 3-5, 2011.
9. Tischler, M.B. and Remple, R.K. “Aircraft and Rotorcraft system Identification,” Engineering Methods with Flight Test Examples, AIAA Publications, Virginia, USA, 2006.
10. Lopez, Mark and Prasad, J.V.R., “Linear Time Invariant Approximations of Time Periodic Systems,” Proceedings of the 38th European Rotorcraft Forum, Amsterdam, Sept. 4-7, 2012.
11. Zhou, K. and Doyle, J.,” Essentials of Robust Control," Prentice Hall, Upper Saddle River, New Jersey, 1998.
12. Vinnicombe, G., “Measuring the Robustness of Feedback Systems”, University of Cambridge, 1992.
13. Lopez, Mark and Prasad, J.V.R, “Fidelity of Reduced Order Time Invartiant Linear (LTI) Models for Integrated Flight and Rotor Control Applications, 69th Annual National Forum of the American Helicopter Society, Pheonix, Arizona, May 21-23, 2013.

9. TABLES

	4/rev Collective Chirp		4/rev Lateral Cyclic Chirp		4/rev Longitudinal Cyclic Chirp	
	LTP	**LTI**	**LTP**	**LTI**	**LTP**	**LTI**
Fx RMS (%)	**4.36**	**2.11**	**5.12**	**3.24**	**4.64**	**2.28**
Fy RMS (%)	**4.33**	**1.96**	**5.16**	**3.28**	**4.35**	**2.04**
Fz RMS (%)	**5.96**	**6.02**	**18.97**	**18.83**	**9.83**	**11.52**
Mx RMS (%)	**5.48**	**5.09**	**5.68**	**4.75**	**4.45**	**4.22**
My RMS (%)	**6.75**	**6.25**	**5.18**	**4.60**	**4.91**	**5.32**
Mz RMS (%)	**5.74**	**5.27**	**17.85**	**17.55**	**4.09**	**4.45**

Table 1. Normalized root mean squared error comparisons for linearized models

10. FIGURES

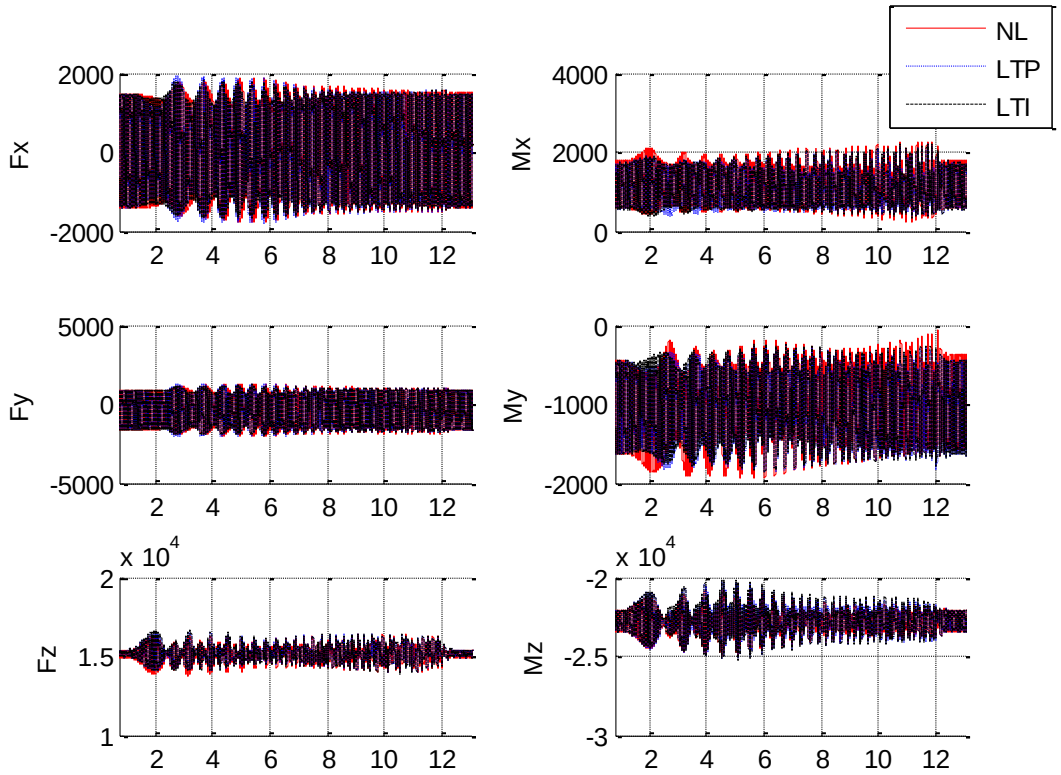

Figure 1. Chirp response to 4/rev collective input

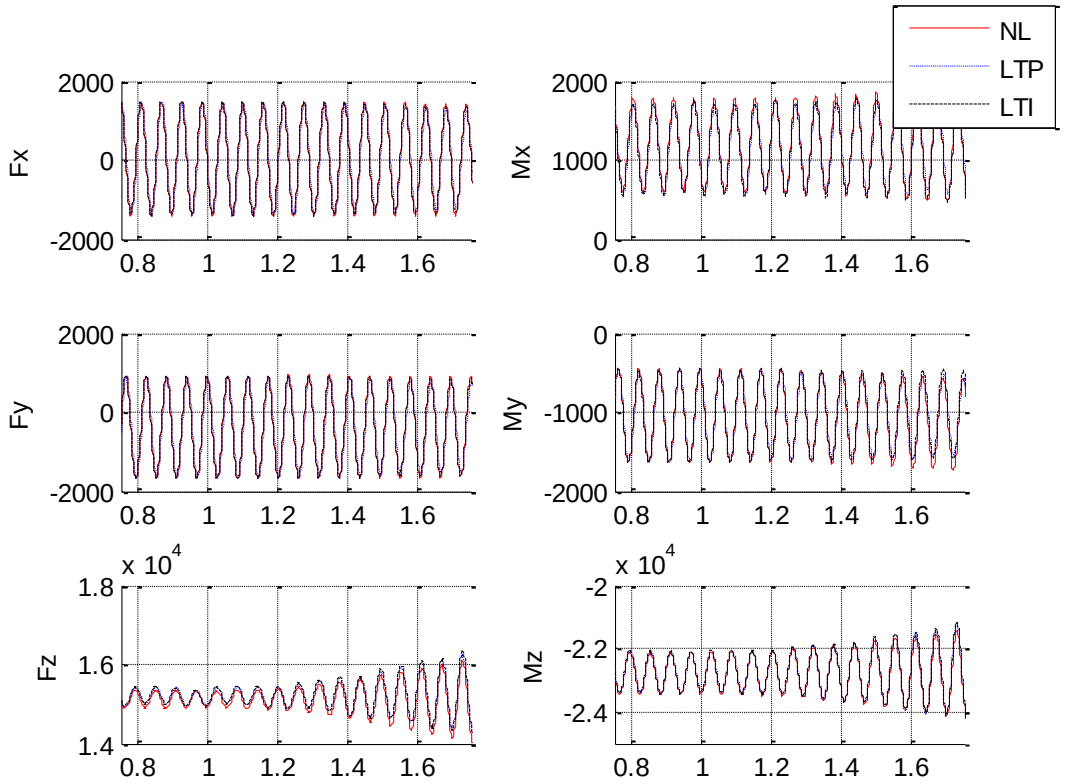

Figure 2. Chirp response to 4/rev collective input (zoom)

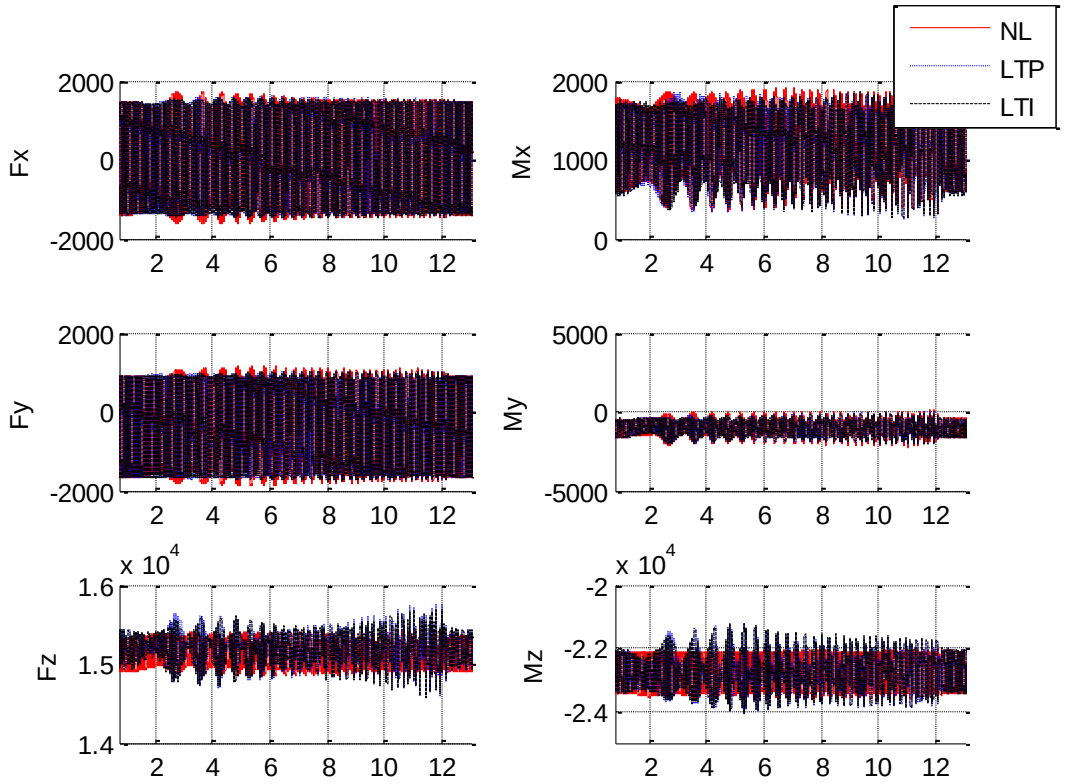

Figure 3. Chirp response to 4/rev lateral cyclic input

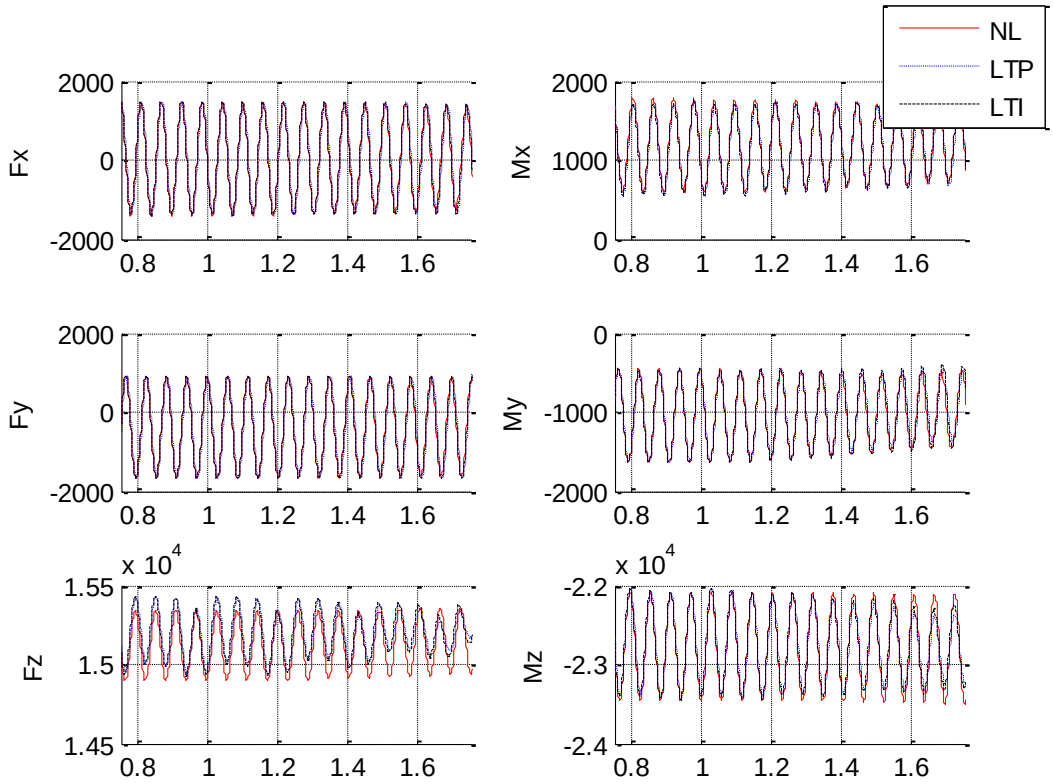

Figure 4. Chirp response to 4/rev lateral cyclic input (zoom)

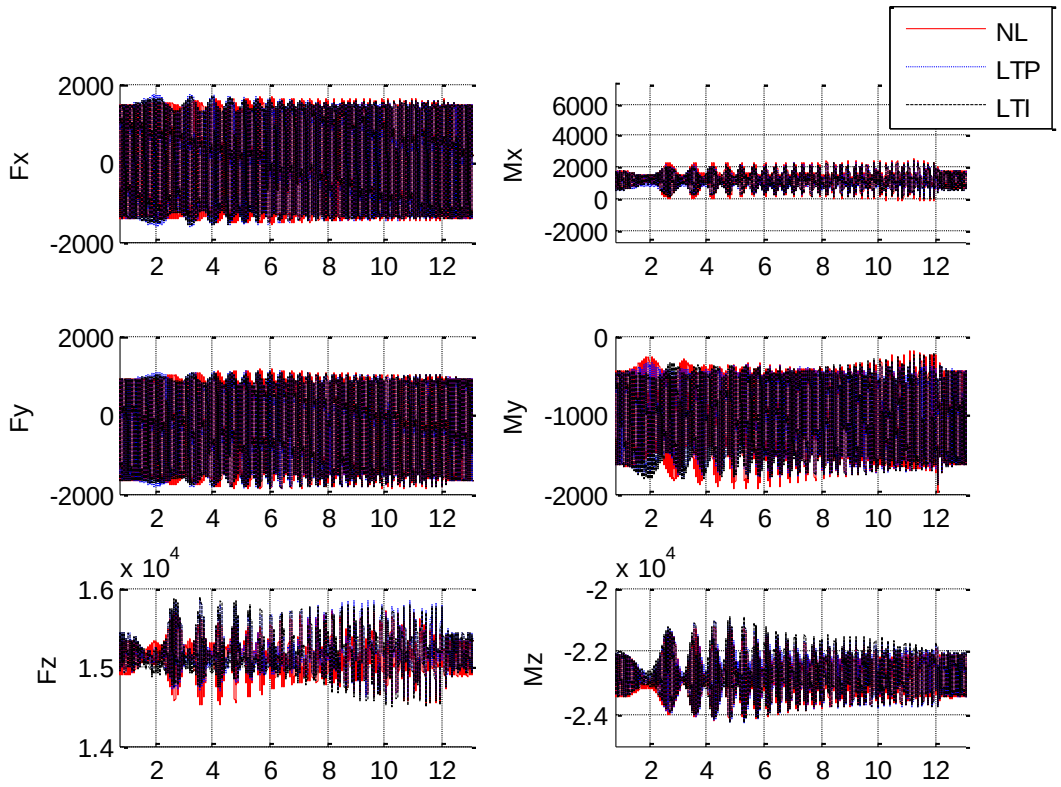

Figure 5. Chirp response to 4/rev longitudinal cyclic input

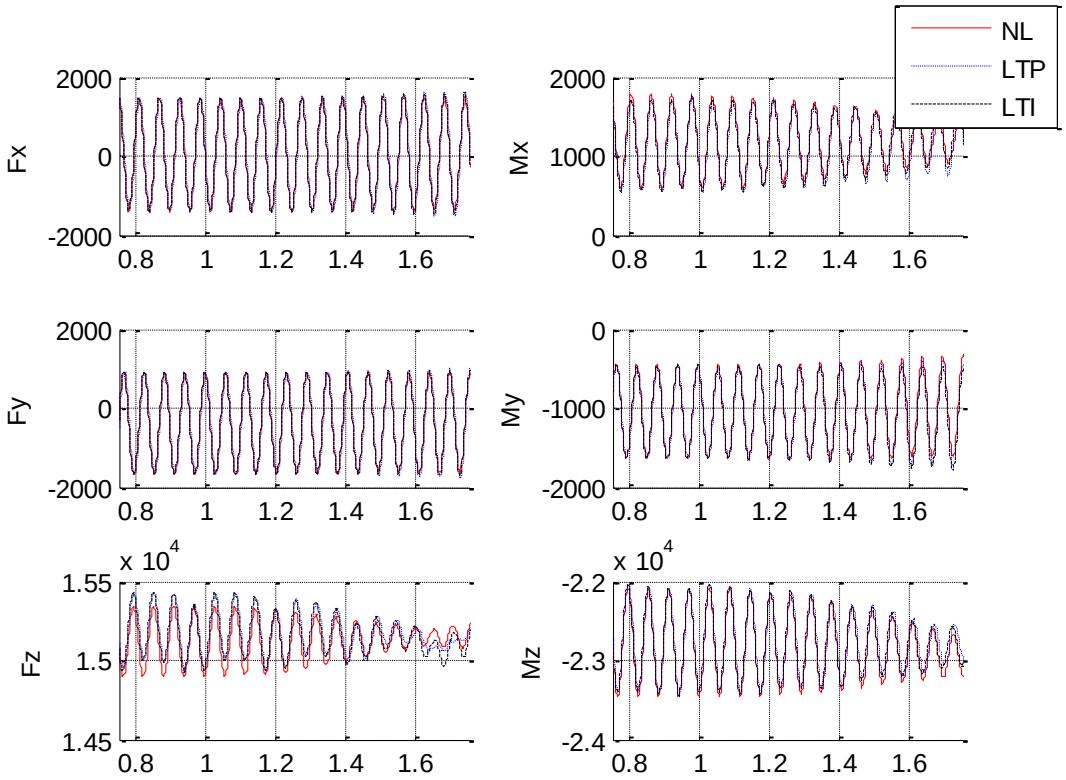

Figure 6. Chirp response to 4/rev longitudinal cyclic input (zoom)

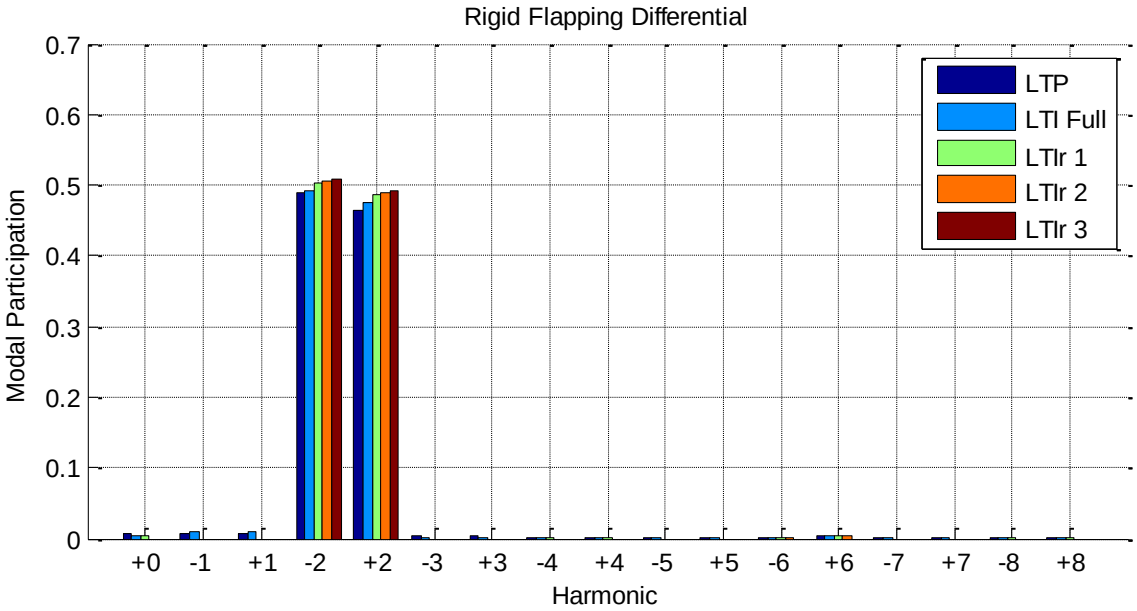

Figure 7. Modal participation for rigid flapping differential, mode 1, advance ratio 0.25

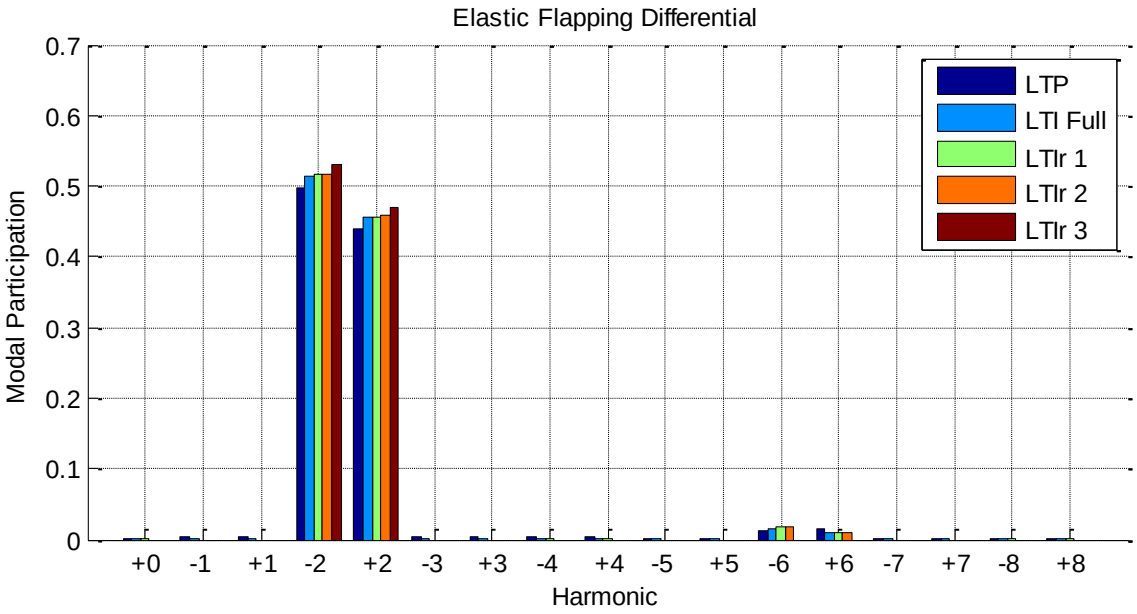

Figure 8. Modal participation for elastic flapping differential, mode 1, advance ratio 0.25

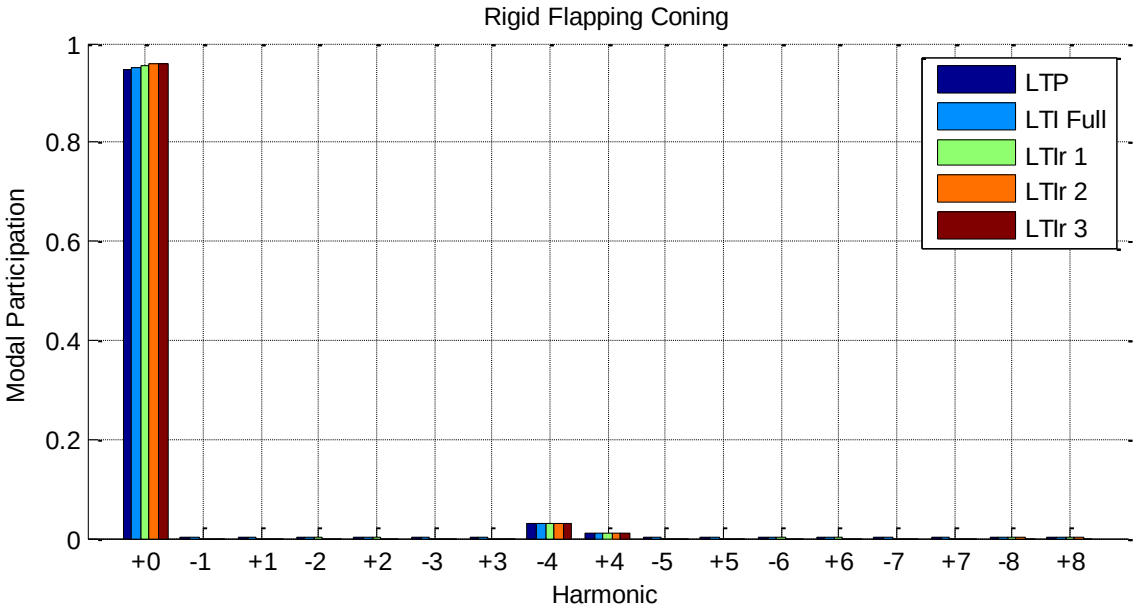

Figure 9. Modal participation for rigid flapping coning, mode 1, advance ratio 0.25

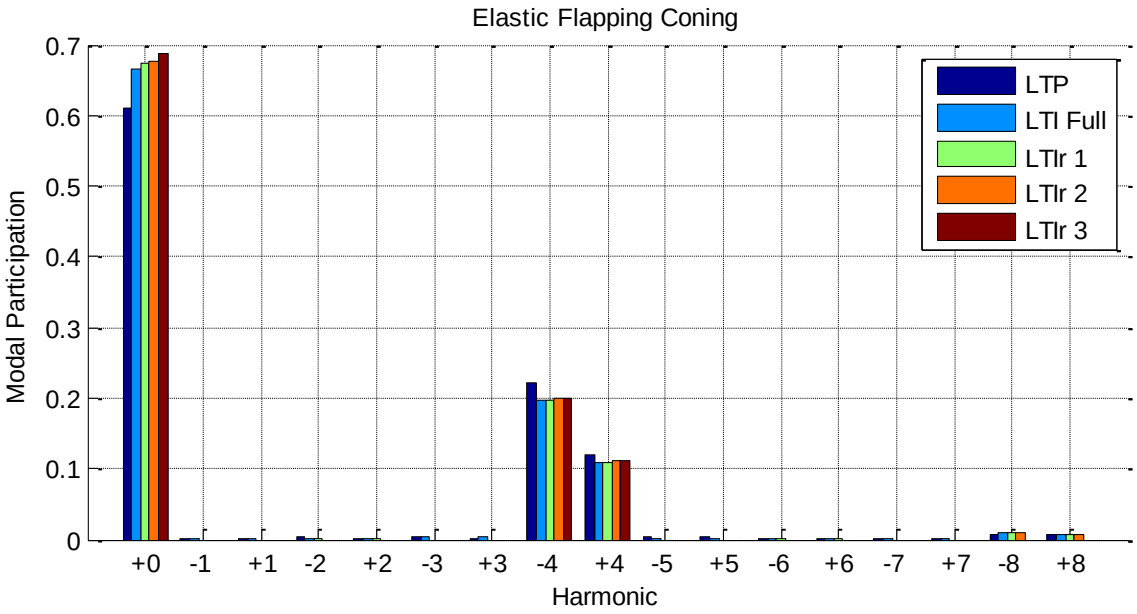

Figure 10. Modal participation for elastic flapping coning, mode 1, advance ratio 0.25

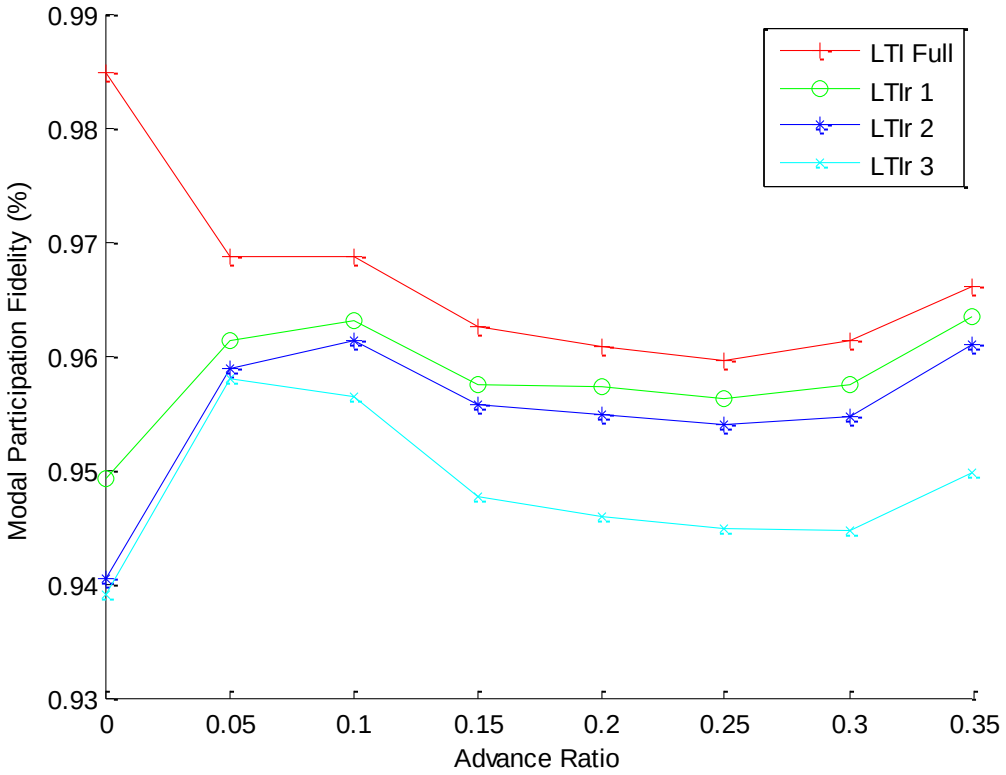

Figure 11. Modal participation fidelity for various LTI reductions

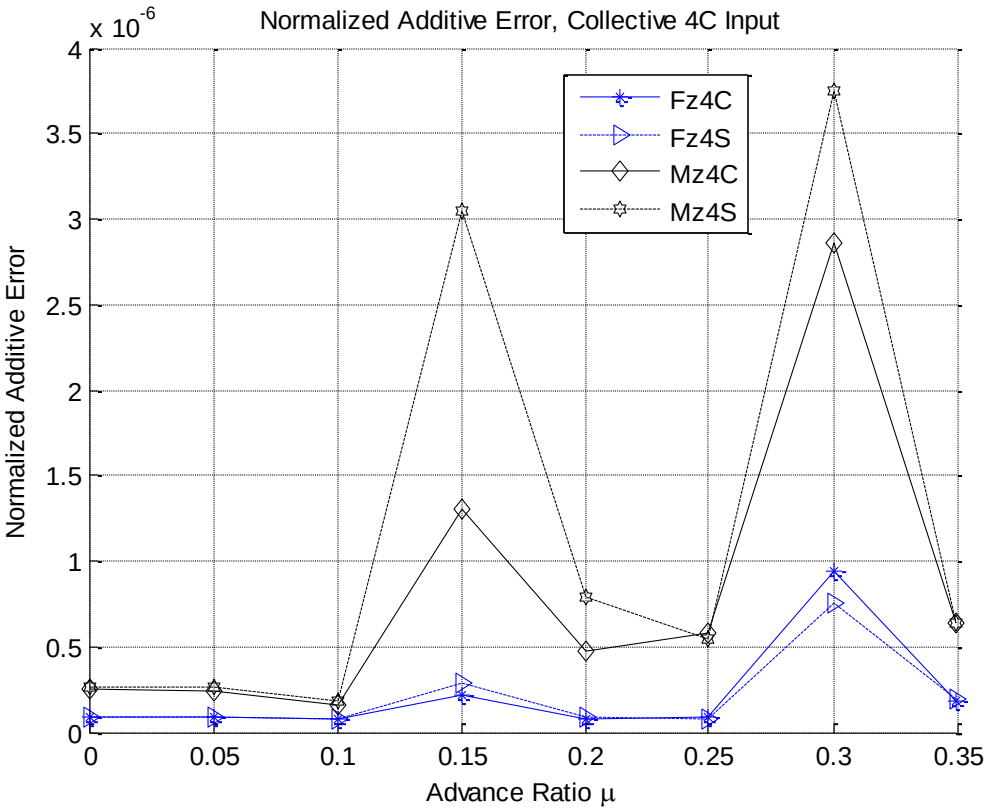

Figure 12. Normalized additive error, collective 4C to direct axis outputs

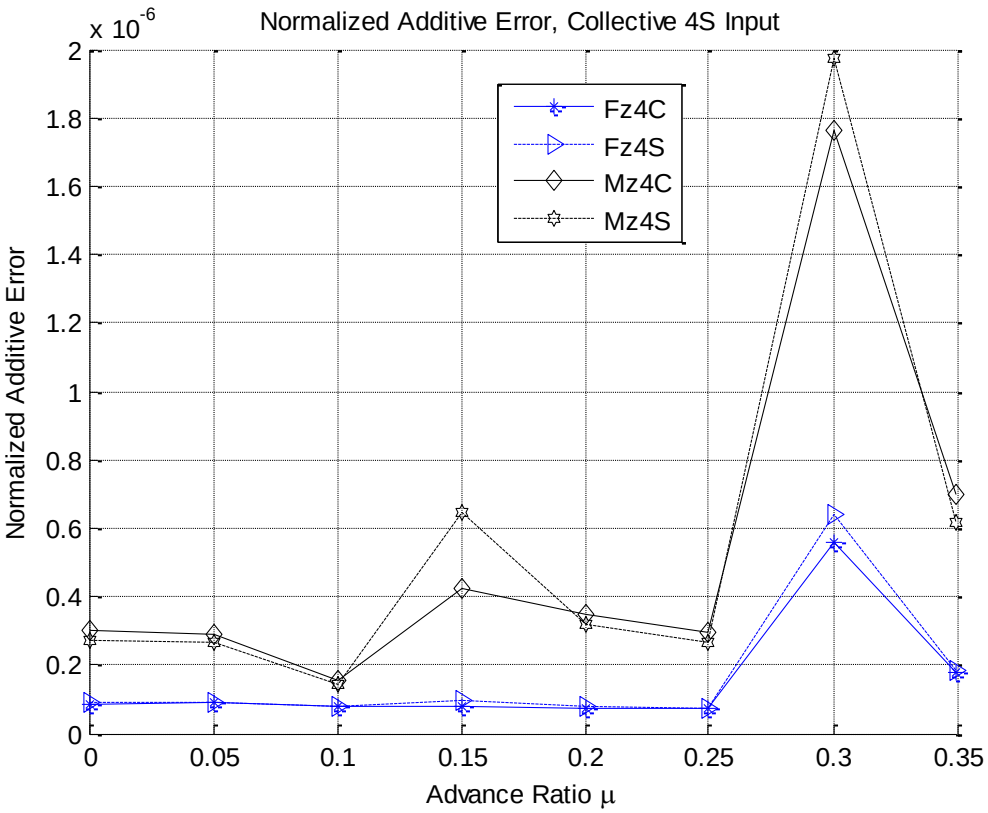

Figure 13. Normalized additive error, collective 4S to direct axis outputs

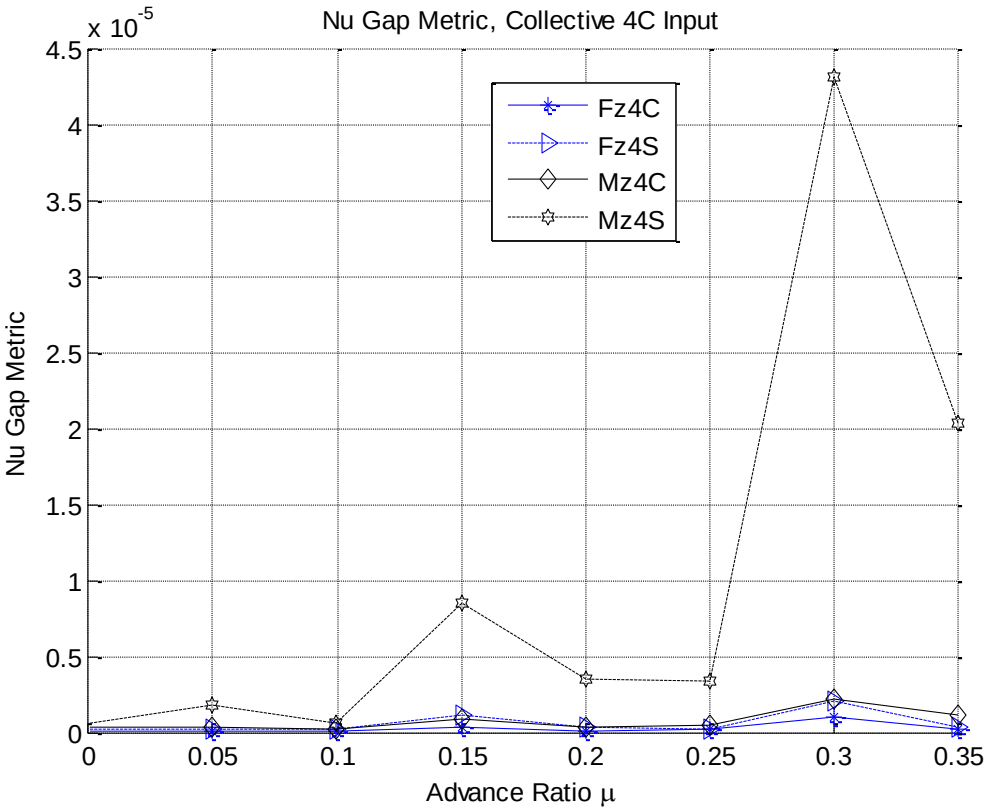

Figure 14. Nu gap metric, collective 4C to direct axis outputs

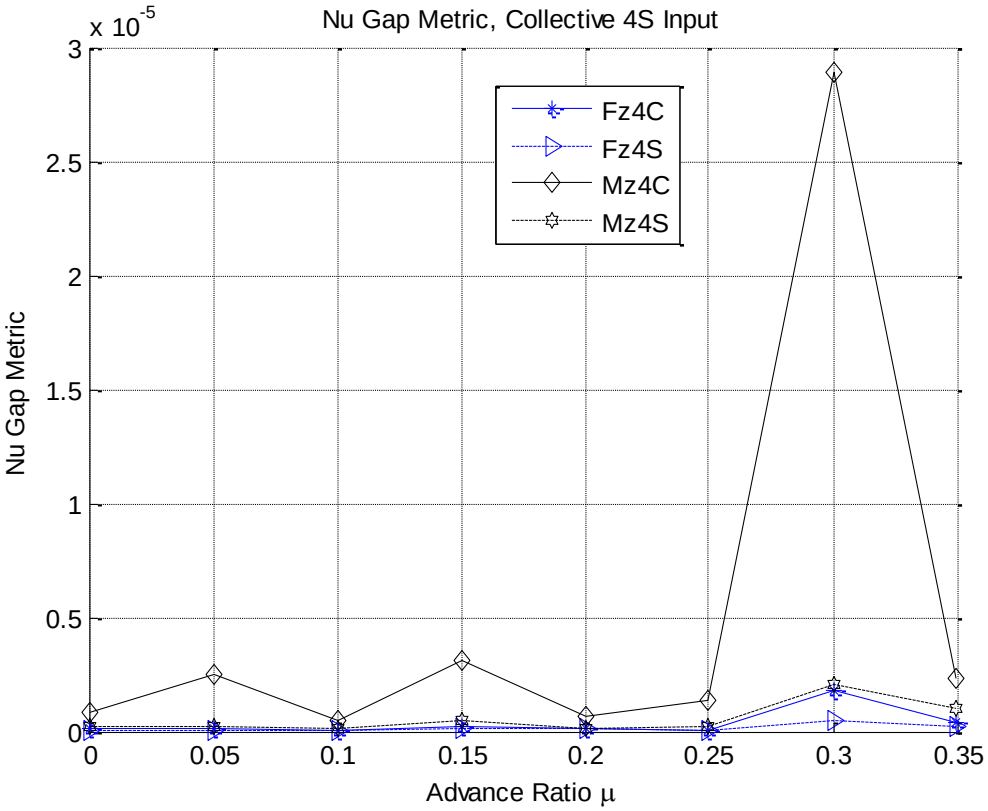

Figure 15. Nu gap metric, collective 4S to direct axis outputs